

Evaluation of hyperoxic gas induced ΔR_1 and ΔR_2^* as MRI biomarkers of tissue oxygenation status in human subjects

J. P. O'Connor^{1,2}, J. H. Naish¹, D. L. Buckley¹, A. Jackson¹, J. C. Waterton^{1,3}, Y. Watson¹, G. A. Buonaccorsi¹, D. M. McGrath¹, S. Cheung¹, S. J. Mills¹, G. C. Jayson², and G. J. Parker¹

¹Imaging Science & Biomedical Engineering, University of Manchester, Manchester, United Kingdom, ²Medical Oncology, Christie Hospital NHS Trust, Manchester, United Kingdom, ³Translational Sciences, AstraZeneca, Macclesfield, United Kingdom

Introduction Change in magnetic resonance signal following inhalation of hyperoxic gas may be quantified to produce biomarkers of tissue oxygenation by measuring changes in longitudinal relaxation rate (R_1)^{1,2} and effective transverse relaxation rate (R_2^*)³. Image contrast in R_1 imaging is due to the paramagnetic effect of dissolved molecular oxygen; whereas contrast in R_2^* – the blood oxygenation level dependent (BOLD) effect – reflects change in tissue levels of deoxygenated haemoglobin species. However, precise mechanisms of hyperoxia-induced R_1 and R_2^* modulation are unclear. We compared the effects of 100% oxygen (O_2) and carbogen (95% O_2 /5% CO_2) inhalation on normal tissue R_1 and R_2^* within the abdomen. It was hypothesised that the two distinct contrast mechanisms may provide complementary information concerning tissue microvasculature.

Study design Ethical approval was obtained. 10 healthy non-smoker volunteers (six female and four male; mean age 32.4 years) were recruited. All experiments took place on a Philips Intera system (Philips Medical Systems, Best, Netherlands) at 1.5 Tesla. Subjects fasted prior to scanning. They then inhaled medical air (21% oxygen) followed by 100% oxygen and then carbogen in the same order and time schedule at 15 l/min through a non re-breathing circuit with reservoir mask.

Data acquisition

- 3D fast field echo (FFE; spoiled gradient echo) images were acquired to produce R_1 maps every 76.8 s using the variable flip angle method⁴. (TR 3.5 ms, TE 0.9 ms, $\alpha = 2^\circ/8^\circ/17^\circ$, 3 averages, FOV 384 x 384 mm², matrix 128 x 128, 33 slices, 3 mm slice thickness). Data were acquired through the upper abdomen.
- 2D multislice T_2^* -weighted dual echo images were acquired over the same anatomical region to enable calculation of tissue R_2^* (TR 548 ms, TE 4.6 & 18.4 ms, $\alpha = 30^\circ$, 5 averages, FOV 375 x 375 mm², matrix 256 x 256, 25 slices, 4 mm slice thickness). Acquisition time was 327 s.

6 R_1 maps and one R_2^* measurement were acquired during each phase of gas inhalation. Transition phases of 8 minutes were interspersed between phases of gas inhalation to allow plateau.

Data analysis Volumes of interest (VOI) were drawn in the spleen, liver, renal cortex and subcutaneous fat. Change in R_1 and R_2^* were calculated where $\Delta R_1 = (R_1(t) - R_1(\text{air}))$ and $\Delta R_2^* = (R_2^*(t) - R_2^*(\text{air}))$. Difference in both R_1 and R_2^* across the group were evaluated using paired samples t-tests. Organ specific ΔR_1 and ΔR_2^* were compared for each subject using Spearman's non-parametric test.

Results Mean tissue $R_1(\text{air})$ and $R_2^*(\text{air})$ were consistent with previous studies¹. Significant increase in R_1 was observed in all organs following inhalation of O_2 and also in the spleen, liver and renal cortex when breathing carbogen (Figure 1A). In the spleen, magnitude of ΔR_1 from baseline was less when breathing carbogen than when breathing oxygen. In the liver, magnitude of ΔR_1 was increased on carbogen. ΔR_1 in the renal cortex showed no significant difference between O_2 and carbogen.

In contrast, no significant ΔR_2^* was seen for any organs when breathing 100 % oxygen. When subjects inhaled carbogen, group mean R_2^* was significantly increased in the spleen ($p < 0.001$), liver ($p = 0.001$), renal cortex ($p = 0.001$) and subcutaneous fat ($p = 0.011$) (Figure 1B). Changes in R_1 and R_2^* are summarised in Table 1. Subject-by-subject ΔR_1 and ΔR_2^* did not correlate for any organ VOI during either O_2 or carbogen inhalation (Figure 2).

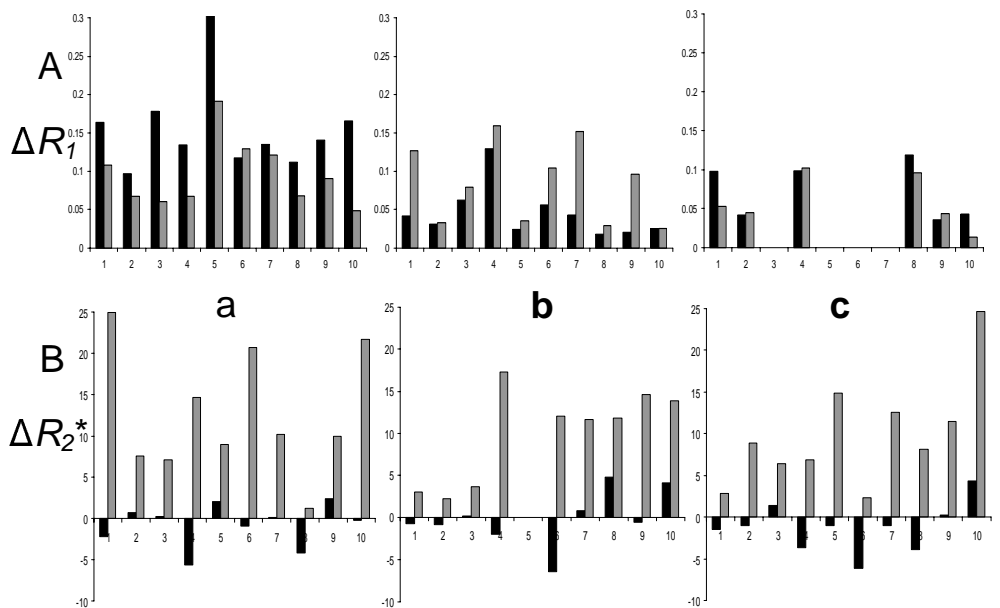
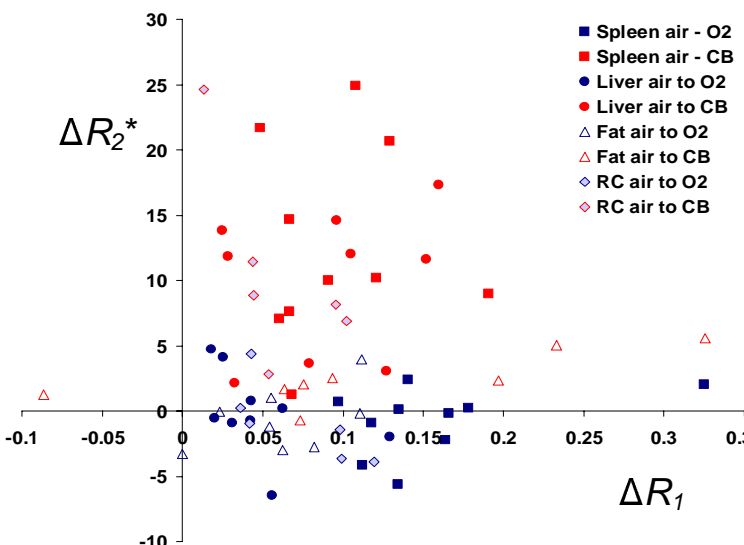


Figure 1 Three tissues are shown (a) spleen, (b) liver and (c) renal cortex in ten subjects. Black shaded bars represent change from air to oxygen; grey bars represent air versus carbogen. Panel (A) shows ΔR_1 (s^{-1}) – black shaded bars represent percentage ΔR_1 from air to oxygen; grey bars represent air to carbogen. Not all subjects had regions of interest in the renal cortex suitable for evaluation. Panel (B) shows ΔR_2^* (s^{-1}). One subject (volunteer 5) did not have an adequate region of interest within the liver.

Table 1 Mean group ΔR_1 and ΔR_2^* when switching from breathing medical air to 100 % oxygen (denoted air versus oxygen) and from baseline to inhalation of carbogen gas (denoted air versus carbogen).

VOI	R_1 data					R_2^* data				
	N	air versus oxygen		air versus carbogen		N	air versus oxygen		air versus carbogen	
		ΔR_1 (s^{-1})	p value	ΔR_1 (s^{-1})	p value		ΔR_2^* (s^{-1})	p value	ΔR_2^* (s^{-1})	p value
Spleen	9	0.157	<0.001	0.095	<0.001	9	-0.750	0.381	12.7	<0.001
Liver	10	0.045	0.002	0.084	0.001	10	-0.096	0.933	10.0	0.001
Fat	9	0.068	<0.001	0.095	0.08	8	-0.685	0.453	2.46	0.011
Renal	6	0.073	0.005	0.059	0.008	10	-1.20	0.229	9.88	0.001



Discussion This study provides further evidence that the image contrast produced by R_1 imaging with carbogen and/or O_2 and R_2^* imaging with carbogen are different but complementary. R_1 mapping with pure oxygen is a relatively simple, reliable technique, with small but measurable signal change. It is postulated that the image contrast induced by O_2 inhalation in R_1 mapping concerns oxygen delivery in arterioles, capillaries and presence in tissue fluid and is influenced by arterial flow, arterial blood volume and tissue metabolism.

A distinct mechanism of tissue contrast is provided by ΔR_2^* . In our study, R_2^* imaging with O_2 did not produce measurable signal change. However, marked but variable ΔR_2^* was detected when carbogen was inhaled. Both techniques show promise as non-invasive biomarkers of tissue oxygenation.

Figure 2 Scatter-plot demonstrating the relationship between ΔR_1 (s^{-1}) and ΔR_2^* (s^{-1}) for each tissue (spleen = squares; liver = circles; fat = triangle outline; renal cortex = grey-filled diamonds). Blue symbols denote transition from air to oxygen (O_2); points are scattered approximated uniformly around the x axis, indicating the lack of significant ΔR_2^* for any tissue while breathing oxygen. Red symbols denote transition from air to carbogen (CB), where significant changes in both R_1 and R_2^* were observed, but no clear relationship was demonstrated between the two parameters.

Acknowledgements This work was supported by Cancer Research UK (grants C19221/A6086 and C237/A6295). JHN and DMMcG are supported by AstraZeneca. ¹RA Jones et al., (2002) MRM 47: 728-35. ²JP O'Connor et al., (2007) MRM 58: 490-6. ³NJ Taylor et al., (2001) JMRI 14: 156-63. ⁴A Haase (1990) MRM 13: 77-89.